INORGANIC CHEMISTRY

FRONTIERS

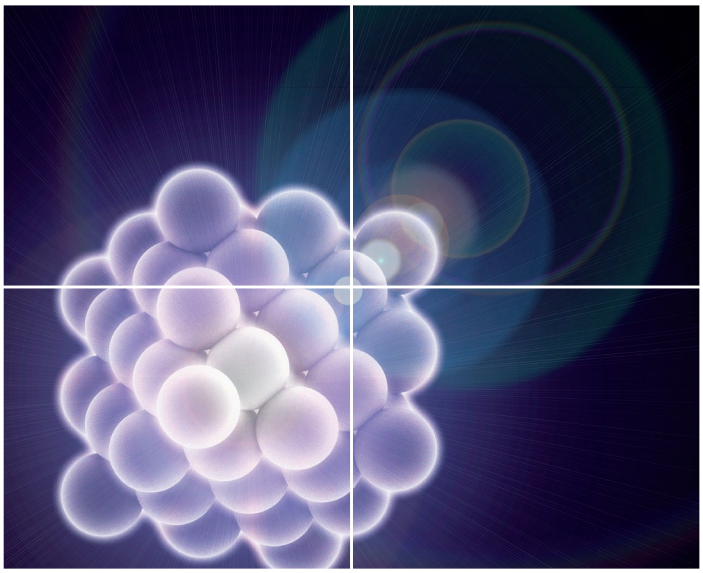

Accepted Manuscript

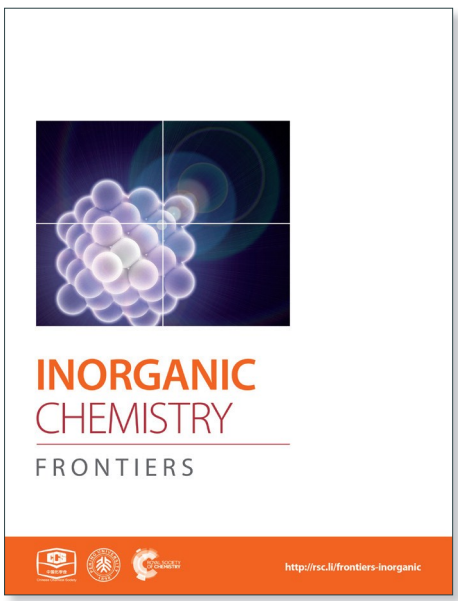

This is an *Accepted Manuscript*, which has been through the Royal Society of Chemistry peer review process and has been accepted for publication.

Accepted Manuscripts are published online shortly after acceptance, before technical editing, formatting and proof reading. Using this free service, authors can make their results available to the community, in citable form, before we publish the edited article. We will replace this *Accepted Manuscript* with the edited and formatted *Advance Article* as soon as it is available.

You can find more information about *Accepted Manuscripts* in the **Information for Authors**.

Please note that technical editing may introduce minor changes to the text and/or graphics, which may alter content. The journal's standard **Terms & Conditions** and the **Ethical guidelines** still apply. In no event shall the Royal Society of Chemistry be held responsible for any errors or omissions in this *Accepted Manuscript* or any consequences arising from the use of any information it contains.

Journal Name

ARTICLE

Flattening sol-gel nanospheres into carbon sheets-intercalated sandwich-nanostructures: cobalt/carbon/cobalt

Received 00th January 20xx,
Accepted 00th January 20xx

DOI: 10.1039/x0xx00000x

www.rsc.org/

Peng Gao,*[a] Yurong Yang,[a,c] Di Bao,[a] Yujin Chen,*[b] Ying Wang,[a] Piaoping Yang*[a] and Xitian Zhang*[d]

It is known that carbon layer's intercalating can reduce and even avoid the breakdown aftermath of the matrix material induced by the expansion in hydrogen storage process. Herein, we provide a general strategy to synthesize uniform cobalt/carbon/cobalt sandwich-like nanosheet-stack (denoted as Co/C/Co), which is difficult to be achieved by conventional one-pot synthetic methods. In this strategy sol-gel nanospheres covered by cobalt^{II}-cobalt^{III} layered double hydroxide (Co^{II}-Co^{III}-LDH) have been constructed firstly and used as the precursor. After a simple post-treatment the sandwich-nanostructures are successfully obtained, which display an extra high capacity, an excellent high-rate capability, and long cycle life. As distinct from the most common structures of carbon-based composites (mixed, wrapped, or anchored models), the resultant materials display a uniform sandwich-like configuration: few-layer carbon sheets conformably intercalates cobalt nanoparticle. This facile strategy can be easily extended to design other metal/carbon/metal sandwich-like nanomaterials.

Introduction

Since the first report in 2004 about an isolated two-dimensional (2D) carbon crystal or graphene (GR) with a single atom thick,[1] it initiated an avalanche of research due to its outstanding optical, electronic, and mechanical properties.[2] Along with it, the attempts to functionalize/decorate/dope 2D carbon have also led to an increasing interest in a large number of modification techniques.[3] More specifically, the preparation of 2D carbon-intercalated structures is a topic of great interest to the catalysis and energy research areas, which has prompted the development of advanced grapheme based materials for energy applications, including supercapacitors, batteries, and fuel cells.[4] However due to their large lattice mismatch and lack of chemical interaction, there is a substantial interfacial energy between them. Thus, when depositing a selected object on the surface of carbon sheet, it often tends to grow only at the defect sites and prefers to form a discontinuous island-like domain to minimize their unfavorable interfaces.[5] Therefore, the formation of a continuous and conformable layer-by-layer structure based on carbon nanosheets remains a great challenge and highly desired. Recently, a "2D chemistry" conception has been provided as a new aspect to the fabrication of layer-by-layer carbon structures. For example: the easily treatable liquid exfoliated GR and reduction of graphene-oxide (rGO) are used to support the deposition of noble metals at organic/water interface, which has been investigated to prepare graphene-based catalysts and electrode materials.[6] However, this method also does not resolve the above problem about their interfaces. Enlightened by the "2D chemistry" method, a new speculation for the decorated carbon nanosheets with a continuous and conformable coverage shell is provided by us in this work: flattening sol-gel hollow nanospheres into carbon sheets-intercalated sandwich-nanostructures. It avoids the collapse effect often induced by the thermal pyrolysis and carbonization process if lamellar sol-gel precursor is directly heat treated, which will only result in the formation of layered composite, not sandwich structure. Fortunately, the above speculation is realized by us through a detailed chemical design, in which cobalt/carbon/cobalt (Co/C/Co) sandwich nanostructures are obtained and display satisfactory electrochemical hydrogen storage property. Firstly, an oil/water sol-gel system containing sphere-like droplets is constructed using cyclohexane as an oil component, Triton X-100 (TX-100, polyoxyethylene octylphenyl ether) as a hydroxyl surfactant and n-butyl alcohol as a co-surfactant. After that layered double hydroxide (LDH) cobalt compounds are introduced, which assembles onto the droplets through the interactions between the hydroxyl groups of itself and the surfactant. The above two steps refer the previous work.[7] Later, the oil component of cyclohexane in the droplet is removed through a forceful centrifugal treatment, resulting in the formation of a carbonaceous sandwich precursor. Finally

[a] Key Laboratory of Superlight Materials and Surface Technology, Ministry of Education, College of Materials Science and Chemical Engineering, Harbin Engineering University, Harbin, Heilongjiang, 150001, P. R. China. E-mail: gaopeng@hrbeu.edu.cn; yangpiaoping@hrbeu.edu.cn
[b] College of Science, Harbin Engineering University, Harbin, Heilongjiang, 150001, P. R. China. E-mail: chenyujin@hrbeu.edu.cn
[c] College of Science, Heihe University, Heihe, Heilongjiang, 164300, P. R. China.
[d] Key Laboratory for Photonic and Electric Bandgap Materials, Ministry of Education, Harbin Normal University, Harbin, Heilongjiang, 150025, P. R. China Email:xtzhangzhang@hotmail.com
Electronic supplementary information available. See DOI: 10.1039/x0xx00000x

through a controlled annealing process a carbon sheets-intercalated cobalt sandwich-structure is obtained assisted by the deoxidizing effect of carbon.

We now report a general strategy to synthesize uniform cobalt/carbon/cobalt sandwich-like nanosheets (denoted as Co/C/Co). The process for the fabrication of superposed Co^{II}-Co^{III}-LDH precursor with a hierarchical structure is schematically illustrated in Scheme 1.

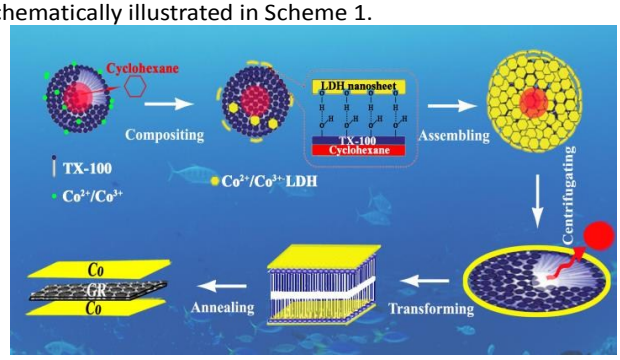

Scheme 1. Schematic illustration of the procedure of the carbon nanosheets-intercalated metal sandwich-structure.

Results and discussion

Structure, Morphology and Composition of the Precursor.

Firstly, cyclohexane oil droplets are well dispersed in a continuous aqueous phase containing the Triton X-100 (TX-100, polyoxyethylene octylphenyl ether) surfactant. Later, cobalt nitrate and hydrogen peroxide are dissolved in the aqueous phase. It is found that its zeta potential value is around +28.2 mV (Fig. S1), confirming that Co^{2+} is well-distributed on the surfaces of the surfactant. After adding ammonia solution, LDH nanosheets form and get deposited and adsorbed on the surfaces of the oil droplets through the hydrogen bonding interactions between the hydroxyl group in TX-100 and that in Co^{II}-Co^{III}-LDH (Fig. S2a inset). On increasing the amount of ammonia solution, more and more LDH crystallites adsorb on the oil droplet surface and assemble as an outer shell, which is hydrogen bonded to the inner shell. At the same time, our dynamic light scattering (DLS) measurements has confirmed the diameter of the spheres changing from 163 nm to 346 nm, as shown in Fig. S2a, which means that the thickness of Co^{II}-Co^{III}-LDH layer is variable. This phenomenon is also observed in the literature.[7] The composition of the LDH is also confirmed by its corresponding XRD measurement (Fig. S2b), which well agrees with the reported literature.[7]

Next, by a high speed centrifugation, the oil phase (cyclohexane) is divided by dint of its different density compared with that of LDH. As shown in Fig. 1a, a large number of superposed lamellar nano-architectures with a diameter of about 450 nm are obtained. Its typical cross-section scanning electron microscope (SEM) image (Fig. 1a inset) shows that a nanoplate is composed of three layers (sandwich-like structure) and the thickness of a single layer is around 10 nm. This special sandwich-like structure is very different from that reported in literature[7] due to the distinct post-treatment of the collected composite precursor in the experiment, in which the composite precursor is only centrifuged, without being washed by any reagent. The above our post-treatment avoids the destruction of the layered composite and assures the formation of the lamellar sandwich structure from the previous sphere-like structure. Transmission electron microscope (TEM) examinations further demonstrate the above result. As shown in Fig. 1b, it is clearly observed that a nanoplate contains different layers. Its related high-resolution transmission electron microscopic (HRTEM) image (Fig. 1b inset) displayed the (110) plane of Co^{II}-Co^{III}-LDH, as expected if its (001) planes are parallel to the nanoplate surface. The fourier transform infrared (FT-IR) spectrum of Co^{II}-Co^{III}-LDH precursors (Fig. 1c) shows a very intense absorption band at 1384 cm^{-1}, corresponding to the absorption peak of intercalated nitrate anions. A broad absorption peak centered at ca. 3380 cm^{-1} can be assigned to the stretching mode of hydrogen-bonded hydroxyl groups, demonstrating the strong stability of the composite. In addition, the Brunauer-Emmett-Teller (BET) area of the precursors is 40.8 $m^2 \cdot g^{-1}$, as shown in Fig. 1d.

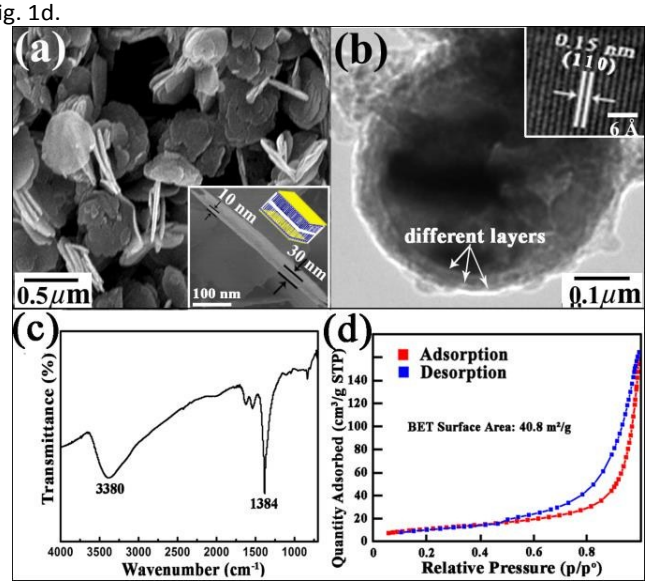

Fig. 1 (a) SEM image of the resulting sample after a high speed centrifugation, the inset is the sample's high-resolution cross-section view; (b) TEM image of the resulting sample, the inset is its corresponding HRTEM image. (c) FT-IR spectrum and (d) N_2 adsorption/desorption isotherm of the superposed Co^{II}-Co^{III}-LDH precursors.

Structure, Morphology and Composition of Co/C/Co Sandwich-nanostructure.

Using the residual surfactant as the carbon source, the sandwich-nanostructured precursor is reduced to their Co/C/Co counterpart. Through a serial of detailed comparison experiments, it is found that in order to avoid the formation of cobalt oxides, the vacuum atmosphere is critical. As shown in Fig. S3 and Table S1, under Ar gas atmosphere cobalt oxide always exist. In contrast, under vacuum atmosphere the precursor is transformed into pure face-centered cubic (*fcc*) cobalt and amorphous carbon at 700 °C, as shown in Fig. S4 and Table S1. The carbon content in the product is about 9.2 wt%, as reported in its ICP-AES result. The change from the surfactant to carbon sheets has been proved by the FT-IR examination. As shown in Fig. S5, the FT-IR result of the resultant Co/C/Co displays a peak at 1370 cm^{-1} due to the plane vibrations of CH and two peaks at 1570 and 3425 cm^{-1} deriving from the hydroxyl groups. Compared with that of the

superposed Co^{II}-Co^{III}-LDH precursors, it is obvous that the surfactant TX-100 has been transformed into carbon-based material. The changes of its composition and structure have also been confirmed by its X-ray photoelectron spectroscopy (XPS) and Raman measurements. As shown in Fig. S6a and b, C 1s peak at 284.6 eV originated from the sp^2-hybridized carbon bond and the Co 2p peaks at 779.2 and 795.5 eV assigned to metallic cobalt[8,9] are observed. The state of carbon element in the product is further studied by Raman examinations. As shown in Fig. S6c, three prominent peaks located at 1344 cm^{-1} (D-band), 1570 cm^{-1} (G-band) and 2688 cm^{-1} (2D-band) are observed, which commensurate with breathing modes of rings and the E_{2g} phonon of sp^2-bonded carbon atoms in two-dimensional hexagonal lattice, respectively.[10] Both XPS and Raman results confirm the process form surfactant to carbon sheets again. Furthermore, it is generally accepted that the character of hierarchical porosity structure has a great influence on its performance in energy storage. Thus the hierarchically structured Co/C/Co is collected for N_2 adsorption/desorption isotherm measurement. The corresponding result (Fig. S6d) displays a desorption hysteresis loop (H_3 type). According to the International Union of Pure and Applied Chemistry (IUPAC) classification, this is often observed for aggregates of plate-like particles giving rise to slit-shaped pores.[11] By calculation single point surface area at p/p°=0.30, a relatively high BET specific surface area (SSA) of 160.4 $m^2 \cdot g^{-1}$ is also obtained. The Barrett-Joyner-Halenda (BJH) pore size distribution plot calculate from desorption branch is shown in the inset of Fig. S6d, which indicates that the Co/C/Co sandwich-nanostructure has both micropores and mesopores, which is attributed to the porous carbon nanosheets intercalated and slit-shaped pores between multiple Co/C/Co architecture, respectively. The large surface area and rich porosity of the hierarchical porous Co/C/Co sandwich-nanostructure should make it a good candidate as electrochemical hydrogen storage materials, considering metal cobalt as a potential hydrogen storage material.

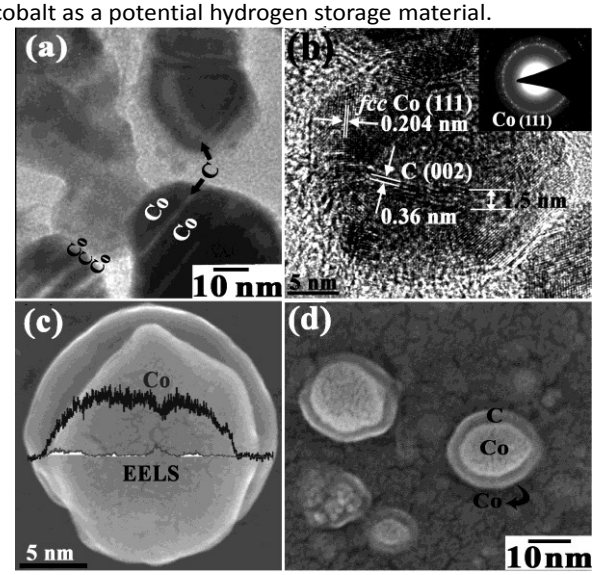

Fig. 2 (a) and (b) Typical TEM and HRTEM images of the Co/C/Co sandwich nanostructures, inset (b) is its corresponding SAED image. (c) and (d) SEM image of the as-obtained nanoparticles, the inset curve in (c) is its EELS result of Co and carbon elements.

The hierarchical nanostructures have been further confirmed through TEM, HRTEM, SAED, SEM and EELS examinations. The TEM results (Fig. 2a and b) and the high-power microscope SEM images (Fig. 2c and d) of the nanostructures confirm that the hierarchical structure is sandwich-like one. Now all the above results prove that the design for Co/C/Co sandwich-nanostructure in Scheme1 has been realized. As shown in Fig. 2b, the (111) lattice plane of *fcc*-Co and (002) lattice plane of carbon intercalated are clearly observed. In addition, it is found that the carbon layer is about 1.5 nm and composed of 5 carbon layers. SAED measurement indicates that the cobalt counterpart in a Co/C/Co nanoparticle is polycrystalline, as shown in Fig. 2b inset. Its SEM image (Fig. 2c) also exhibits the sandwich-structure with a 25 nm diameter, in which EELS curve demonstrates the composition of the sandwich-structure and that Co and C elements take up its whole regions. The presence of carbon nanosheets intercalation not only strengthens the hierarchical structure, but also prevents the nanoparticles from complete agglomeration, leaving large interspaces between them, which provide abundant diffusion channels for guest moleculors.

Electrochemical Hydrogen Storage Properties.

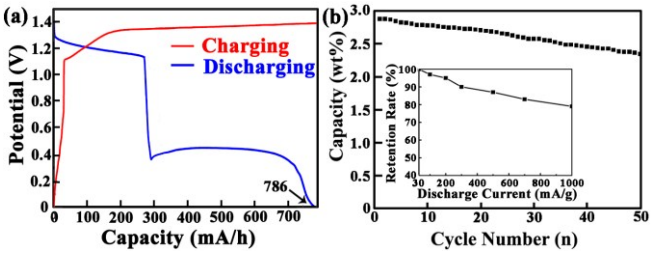

Fig. 3 (a) Electrochemical hydrogen storage charging-discharging curves of the as-obtained product at a current density of 30 mA/g; (b) Cycle performances and retention rate at various discharge hydrogen densities of the Co/C/Co sandwich-nanostructure.

To further investigate the hydrogen storage ability of the Co/C/Co sandwich-nanostructure, its electrochemical hydrogen storage capacity at a 30 mA/g current density is firstly tested, as shown in Fig. 3a. In the charge process, one charge plateau appears at about 1.36 V, which can be ascribed to the reaction of Co/C/Co→Co/C/Co-H_x, similar to that reported in literatures.[12,13] At the same time, a mass of gas bubbles have also been observed in our experiments. All the above phenomena prove the production of hydrogen in the electrochemical process. In the discharge curve, two obvious plateaus are observed at 1.20 V and 0.43 V, respectively, which suggests that different hydrogen desorption sites exist in the product. Lower discharge plateaus appearing at about 0.43 V should be attributed to the desorption of hydrogen adsorbed on the surface of the nanocomposite, which has been pointed out in literatures.[14,15] The discharge plateau appearing at about 1.20 V is comparable to that of other Co based alloys,[16] which is due to the reaction of Co/C/Co-H_x→Co/C/Co. It is also noted that the balanced lengths of both charge and discharge plateaus indicate the excellent reversibility and columbic efficiency of the electrode. Furthermore, cycle performances demonstrate that the as-prepared Co/C/Co sandwich-

nanostructure own satisfactory stability as electrochemical hydrogen storage materials. Fig. 3b shows the cycle stability of the product at a discharge current density of 30 mA/g. It is clear that the composite achieves a maximum discharge capacity as high as 786 mAh/g (2.88 wt% hydrogen), which is about 1.82 times of that of pure Co nanoparticles[17] and close to the theoretical hydrogen storage capacities of individual metal Co.[17] Importantly, even after 50 cycles, the discharge capacity still remains at 667 mAh g^{-1} (2.44 wt% hydrogen). Compared with traditional AB_5 type,[18,19] AB_2 type,[20] AB type[21] and Mg-based alloy[22,23] hydrogen storage materials, the as-prepared Co/C/Co sandwich-nanostructure displays a much higher discharge capacity and cycling stability, which are due to that the intercalated carbon sheets tightly envelop the Co nanoparticles to protect and restrict them just like a three-layered sandwich. Also the carbon sheets as a buffer layer conveniently allow bypassing the nanostructure's collapse that would inevitably arise in the hydrogen absorption/desorption process. Our observation of the maintained nanostructure after hydrogen absorption/desorption cycles demonstrate the above point. Additionally, the Co/C/Co sandwich-nanostructure also exhibit good electrochemical hydrogen storage performances at high current densities. To further test its cyclability under various high rates, discharge apacities versus current densities from 30 to 1000 mA are examined. As shown in Fig. 3b, the discharging capacity varies from 786 to 636.7 mAh/g. The discharging capacity curves still maintain satisfactory kinetic feature at high rates, indicating a facile charge transport process. Notably, the retention of the as-obtained nanocomposites is up to 95% at the discharging hydrogen density of 200 mA/g, which is much higher than the previous results.[24]

We attribute the excellent hydrogen storage performance of the product to its unique hierarchical architecture. Firstly, in the as-obtained open hierarchical structure, the interlayer spacing between the layers can be easily filled with electrolyte, ensuring a high surface area comes into effective contact with the electrolyte, facilitating transportation of a large flux of hydrogen storage. Secondly, the porous sandwich-nanostructure offers a very short effective diffusion distance for hydrogen, resulting in an enhanced rate performance. Thirdly, the thin carbon layers, as a conducting coating on cobalt nanoparticles, not only significantly enhance the electrical conductivity of the material, but also supply continuous conductive paths between Co particle and carbon sheets. Last but not least, each of the spaces between the carbon sheets, provides elastic buffer spaces to accommodate the volume changes during hydrogen insertion and extraction, which attributes to excellent cyclability and high rates retention ability.

Finally, cyclic voltammogram curve (CV) is carried out to further investigate the electrochemical hydrogen adsorption-desorption behaviors of the product, as shown in Fig. S7. The main CV feature of the sample shows two remarkable anodic current peaks, which is different from the result of previous reports only exhibiting one pair of peak.[25] In the reversed scan, two strong oxidation peaks center at -0.96 V and -0.20 V, which are far from the equilibrium potentials of pure Co and carbon materilas.[26,27] The potential position and feature of the anodic peak at -0.96 V agree with the discharge potecial at 1.2 V, which belongs to the electrochemical oxidation of hydrogen in crystal lattice, as reported in literatures.[27-29] The current peak appearing at about -0.20 V is comparable to the discharge plateaus at 0.43 V in the hydrogen desorption process, which is due to the electrochemical oxidation of hydrogen adsorbed on the surface of the electrode material and frequently observed for the electrochemical hydrogen storage electrodes.[30,31] So the reversible CV peaks observed here are ascribed to the quasi-reversible electrochemical reaction:

$$Co/C/Co+xH_2O+xe^- \leftrightarrow Co/C/Co\text{-}Hx+xOH^-$$

Conclusions

In summary, we demonstrate a general strategy for synthesis of metal/carbon/metal sandwich-like nanoprticles, which can avoid the substantial interfacial tensions that would be inevitably engendered if direct growth of metal nanoparticles on carbon sheet. The as-prepared Co/C/Co sandwich-nanostructures show a high capacity, an excellent rate capability and good cycling stability as anticipated by us.

Experimental Section

Synthesis of the Co^{II}-Co^{III}-LDH precursor. The O/W emulsion consisted of cyclohexane (5 mL), TX-100 surfactant (20 mL) and n-butyl alcohol co-surfactant (10 mL) as the oil phase and water (250 mL). The mixture was vigorously stirred and 0.01 mol $Co(NO_3)_2{\cdot}6H_2O$ and of hydrogen peroxide solution (1 mL, 30%) were dissolved in the water phase. Then, with a stirring speed of 60 rpm, 10 wt% ammonia aqueous solution was added into the emulsion at a rate of 4 mL·min^{-1} to a give a pH value at 9.5. The reaction was allowed to proceed at ambient temperature for 9 hours (h), after which the suspension was centrifuged and collected. For subsequent characterization, the product was washed with double distilled water and ethanol and then dried at 60 °C for 10 h.

Synthesis of the Co/C/Co sandwich-structure. The unwashed composite precursor (containing residual surfactant) was collected and calcinated at 700 °C for 4 h in a vacuum atmosphere. This treatment ensured that the surfactant decomposed and carbonized to amorphous carbon.

Characterization. The crystallographic structures of the materials were determined using a powder XRD system (TTR-III, Japan) equipped with Cu Kα radiation (λ=0.15406 nm). The scan rate of 10° min^{-1} was used to record the patterns in the range of 10-70°. The products were observed under a SU8000 cold emission field scanning electron microanalyser (Hitachi, Japan) operated at 10 kV for their microstructures. Transmission electron microscope (TEM) images and the high-resolution transmission electron microscopic (HRTEM) images of the nanostructures were taken using a JEOL HRTEM (JEM2010 electron microscope) at 200 kV accelerating voltage. Fourier transform infrared (FT-IR) spectra were recorded with 2 cm^{-1} spectral resolution using a PerkinElmer Spotlight spectrometer. Dynamic light scattering (DLS) and zeta potential measurements were performed with a Malvern Zetasizer NS90 equipped with a He/Ne laser (633 nm wavelength). Furthermore, N_2 adsorption/desorption measurements were measured at a liquid

nitrogen temperature (77 K) using a Micromeritics ASAP 3020 instrument. The specific surface area was calculated by the Brunauer-Emmett-Teller (BET) method. The X-ray photoelectron spectroscopy (XPS) measurements were performed by using a PHI 5700 ESCA system with a monochromatic Al-Kα (1486.6 eV) radiation source and a hemisphere detector. Moreover, in order to determinate Co and C element content in the composites, using 0.1 M HNO_3 to dissolve the composites and its dissolved solution was filtered and analyzed by inductive coupled plasma atomic emission spectrometer (ICP-AES) measurement (Thermo Elemental, IRIS Intrepid II XSP).

Electrochemical Hydrogen Storage Measurements. The hydrogen charging and discharging curves were measured in a two-electrode test cell by a LAND battery test instrument (CT2001A), which contains one piece of positive electrode and one piece of negative electrode, and the electrolyte was 6 M KOH aqueous solution. The negative electrode was composed of 85 wt% of the as-obtained powder, 10 wt% acetylene black. The positive electrode material consisted of 80 wt% nickel hydroxide, 15 wt% Co. Each of the positive and negative electrode material was mixed with 5 wt% PTFE and coated on a 1 cm^2 Ni-foam. The electrode plates were pressed at a pressure of 50 $kg \cdot cm^{-2}$ for 30 s. The CV measurement was performed by using an electrochemical workstation (CHI 660E) of three-electrode test cell. The cell was consisted of the as-obtained compounds as the working electrode, a metal platinum gauze as the counter electrode and a Hg/Hg_2Cl_2 electrode as the reference electrode, and the electrolyte was 6 M KOH. The scan range was between -1.2 V and 0 V vs Hg/Hg_2Cl_2, and the scan started from the open circuit potential and then along the negative direction at a scan rate of 10 $mV \cdot s^{-1}$.

Acknowledgements

We thank the Program for NCET in University (NCET-13-0754), the Natural Science Foundation of China (Grant No. 51272050 and 51072038); the fundamental research funds for the central universities (No. HEUCF2016); Harbin Sci-tech innovation foundation (RC2012XK017012); Harbin Youth Fund (RC2014QN017004); Youth Fund of Heilongjiang Province (QC2014C006) for the financial support of this research; the Open Project Program of Key Laboratory for Photonic and Electric Bandgap Materials, Ministry of Education, Harbin Normal University (PEBM201301).

Notes and references

1 K. S. Novoselov, A. K. Geim, S. V. Morozov, D. Jiang, Y. Zhang, S. V. Dubonos, I. V. Grigorieva and A. A. Firsov, *Science*, 2004, **30**, 666.

2 a) I. Vlassiouk, S. Smirnov, I. Ivanov, P. F. Fulvio, S. Dai, H. Meyer, M. Chi, D. Hensley, P. Datskos and N. V. Lavrik, *Nanotechnology*, 2011, **22**, 1; b) C. M. Weber, D. M. Eisele, J. P. Rabe, Y. Liang, X. Feng, L. Zhi, K. Mullen, J. L. Lyon, R. Williams, D. A. Vanden Bout and K. J. Stevenson, *Small*, 2010, **6**, 184; c) K. S. Novoselov, A. K. Geim, S. V. Morozov, D. Jiang, M. I. Katsnelson, I. V. Grigorieva, S. V. Dubono and A. A. Firsov, *Nature*, 2005, **438**, 197.

3 a) J. A. Robinson, M. Hollande, M. LaBella, K. A.Trumbull, R. Cavalero and D. W. Snyder, *Nano Lett.*, 2011,**11**, 3875; b) A. Mishchenko, J. S. Tu, Y. Cao, R. V. Gorbachev, J. R. Wallbank, M. T. Greenaway, V. E. Morozov, S. V. Morozov, M. J. Zhu, S. L. Wong, F. Withers, C. R. Woods, Y. J. Kim, K. Watanabe, T. Taniguchi, E. E. Vdovin, O. Makarovsky, T. M. Fromhold, V. I. Fal'ko, A. K. Geim, L. Eaves and K. S. Novoselov, *Nat. Nanotech.,* 2014, **9**, 808.

4 a) V. H. Rodrigues de Souza, M. M. Oliveira and A. J. Gorgatti Zarbin, *J. Power Sources*, 2014, **260**, 34; b) P. V. Kamat, *J. Phys. Chem. Lett.,* 2010, **1**, 520; c) J. M. Yuk, K. Kim, B. N. Alemán, W. Regan, J. H. Ryu, J. Park, P. Ercius, H. M. Lee, A. P. Alivisatos, M. F. Crommie, J. Y. Lee and A. Zettl, *Nano Lett.*, 2011, **11**, 3290.

5 a) X. Huang, X. Y. Qi, F. Boey and H. Zhang, *Chem. Soc. Rev*., 2012, **41**, 666; b) Q. J. Xiang ,J. G. Yu and M. Jaroniec, *Chem. Soc. Rev*. 2012, **41**, 782; c) H. L. Wang and H. J. Dai, *Chem. Soc. Rev*., 2013, **42**, 3088; d) Z. S. Wu, G. M. Zhou, L. C. Yin, W. Ren, F. Li and H. M. Cheng, *Nano Energy,* 2012, **1**, 107; e) X. Li, W. Qi, D. Mei, M. L. Sushko, I. Aksay and J. Liu, *Adv. Mater*., 2012, **24**, 5136; f) D. H. Wang, R. Kou, D. Choi, Z. G. Yang, Z. M. Nie, J. Li, L. V. Saraf, D. H. Hu, J. G. Zhang, G. L. Graff, J. Liu, M. A. Pope and I. A. Aksay, *ACS Nano*, 2010, **4**, 1587.

6 a) S. J. Hoseini, M. Dehghani and H. Nasrabadi, *Catal. Sci. Tech.,* 2014, **4**, 1078; b) K. Bramhaiah and N. S. John, *RSC Adv.,* 2013, **3**, 7765; c) X. Zan, Z. Fang, J. Wu, F. Xiao, F. Huo and H. Duan, *Biosens. Bioelectron*., 2013, **49**, 71; d) M. M. Gudarzi and F. Sharif, *Soft Matter,* 2011, **7**, 3432; e) S. Biswas and L. T. Drzal, *Nano Lett*., 2009, **9**, 167; f) R. V. Salvatierra, S. H. Domingues, M. M. Oliveira and A. J. G. Zarbin, *Carbon*, 2013, **57**, 410.

7 J. Sun, H. M. Liu, X. Chen, D. G. Evans and W. S. Yang, *Nanoscale*, 2013, **5**, 7564.

8 M. C. Biesinger, B. P. Payne, A. P. Grosvenor, L. M. Lau, A. R. Gerson and R. S. C. Smart, *Appl. Surf. Sci.,* 2011, **257**, 2717.

9 X. A. Li, X. J. Han, Y. C. Du and P. Xu, *J Magn. Magn. Mater*., 2011, **323**, 14.

10 R. J. Tseng, C. O. Baker, B. Shedd, J. X. Huang, R. B. Kaner, J. Y. Ouyang and Y. Yang, *Appl. Phys. Lett*., 2007, **90**, 053101.

11 K. S. W. Sing, D. H. Everett, R. A. W. Haul, L. Moscou, R. A. Pierotti and J. Rouquerol, *Pure Appl. Chem*., 1985, **57**, 603.

12 Y. L. Cao, W. C. Zhou, X. Y. Li, X. P. Ai, X. P. Gao and H. X. Yang, *Electrochim. Acta*, 2006, **51**, 4285.

13 Y. H. Zhang, L. F. Jiao, H. T. Yuan, Y. Y. Zhang, L. Liu and Y. J. Wang, *Int. J. Hydrogen Energy*, 2008, **33**, 1317.

14 Z. W. Lu, S. M. Yao, G. R. Li, T. Y. Yan and X. P. Gao, *Electrochim. Acta*, 2008, **53**, 2369.

15 G. P. Dai, C. Liu, M. Liu, M. Z. Wang and H. M. Cheng, *Nano Lett*., 2002, **2**, 503.

16 D. W. Song, Y. J. Wang, Q. H. Wang, Y. P. Wang, L. F. Jiao and H. T. Yuan, *J. Power Sources*, 2010, **195**, 7115.

17 S. R. Chung, K. W. Wang and T. P. Perng, *J. Electrochem. Soc*., 2006, **153**, 1128.

18 B. Liao, Y. Q. Lei, L. X. Chen, G. L. Lu, H. G. Pan and Q. D. Wang, *J. Power Sources*, 2004, **129**, 358.

19 T. Kohno, H. Yosid and F. Kawashima, *J. Alloys Compd*., 2000, **311**, 5.

20 M. Y. Song, D. Ahn, I. H. Kwon and S. H. Chough, *J. Electrochem. Soc*., 2001, **148**, 1041.

21 H. Yukawa, Y. Takahashi and M. Morinaga, *Mater. Sci*., 1999, **14**, 291.

22 Q. F. Tian, Y. Zhang, L. X. Sun, F. Xu, Z. C. Tan and H. T. Yuan, *J. Power Sources*, 2006, **158**, 1463.

23 W. Liu, Y. Lei, D. Sun, J. Wu and Q. D. Wang, *J. Power Sources*, 1996, **58**, 243.

24 a) S. Q. Yang, P. Gao, D. Bao, Y. J. Chen, L. Q. Wang,; P. P. Yang, G. B. Li and Y. Z. Sun, *J. Mater. Chem. A,* 2013, **1**, 6731; b) D. Bao, P. Gao, X. D. Shen, C. Chang, L. Q. Wang, Y. Wang, Y. J. Chen, X. M. Zhou, S. C. Sun, G. B. Li and P. P. Yang, *ACS Appl. Mater. Interfaces*, 2014, **6**, 2902; c) C. Chang, P. Gao, D. Bao, L. Q. Wang, Y. Wang, Y. J. Chen, X. M. Zhou, S. C. Sun, G. B. Li and P. P. Yang, *J. Power Sources*, 2014, **255**, 318; d) Y. J. Chen,

Q. S. Wang, C. L. Zhu, P. Gao, Q. Y. Ouyang, T. S. Wang, Y. Ma and C. W. Sun, *J. Mater. Chem*., 2012, **22**, 5924.
25 D. Wang, X. P. Ai and H. X. Yang, *Chem. Mater*., 2004, **16**, 5194.
26 W. T. Tan, E. B. Lim and J. K. Goh, *J. Solid State Electrochem.*, 2005, **9**, 30.
27 Y. Liu, Y. J. Wang, L. L. Xiao, D. W. Song, Y. P. Wang, L. F. Jiao and H. T. Yuan, *Electrochim. Acta*, 2008, **53**, 2265.
28 V. Lavrentiev, H. Naramoto, K. Narumi, S. Sakai and P. Avramov, *Chem. Phys. Lett*., 2006, **423**, 366.
29 P. Gao, Y. Wang, S. Q. Yang, Y. J. Chen, Z. Xue, L. Q. Wang, G. B. Li and Y. Z. Sun, *Int. J. Hydrogen Energy*, 2012, **37**, 17126.
30 S. Sakai, H. Naramoto, P. V. Avramov, T. Yaita, V. Lavrentiev, K. Narumi, Y. Baba and Y. Maeda, *Thin Solid Films*, 2007, **515**, 7758.
31 P. Gao, S. Q. Yang, Z. Xue, G. B. Liu, G. L. Zhang, L. Q. Wang, G. B. Li, Y. Z. Sun and Y. J. Chen, *J. Alloys Compd*., 2012, **539**, 90.